Forward and backward stimulated Brillouin scattering of crossed laser beams

C. J. McKinstrie and E. A. Startsev
Department of Mechanical Engineering, University of Rochester, Rochester, New York 14627
and Laboratory for Laser Energetics, 250 East River Road, Rochester, New York 14623
(Received 8 March 1999)

The simultaneous forward and backward stimulated Brillouin scattering (SBS) of crossed laser beams is studied in detail. Analytical solutions are obtained for the linearized equations governing the transient phase of the instability and the nonlinear equations governing the steady state. These solutions show that backward SBS dominates the initial evolution of the instability, whereas forward SBS dominates the steady state. The analysis of this paper is verified by numerical simulation. [S1063-651X(99)02711-7]

PACS number(s): 52.35.Mw, 52.35.Nx, 52.40.Nk, 42.65.Es

I. INTRODUCTION

Stimulated Brillouin scattering (SBS) in a plasma is the decay of an incident (pump) light wave into a frequency-downshifted (Stokes) light wave and an ion-acoustic (sound) wave [1]. It is important in direct [2] and indirect [3] inertial-confinement-fusion (ICF) experiments because it scatters the laser beams away from the target, thereby reducing the energy available to drive the compressive heating of the nuclear fuel.

The SBS of an isolated beam has been studied in detail. Backward SBS was studied in numerous early papers, and near-forward, sideward, and near-backward SBS were studied in some recent papers [4–8]. However, because beams overlap in the coronal plasma surrounding the nuclear fuel, it is also important to analyze SBS (and other parametric instabilities) driven by two (or more) crossed beams. For some scattering angles, the SBS geometries allow the pump waves to share daughter waves [9–11]. Because the growth of these daughter waves is driven by two pump waves (rather than one), the growth rates associated with these scattering angles are higher than the growth rates associated with other scattering angles. Such is the case for forward and backward SBS, in which the Stokes wave vectors bisect the angle between the pump wave vectors.

In this paper we study the simultaneous forward and backward SBS of crossed beams. The outline of the paper is as follows. In Sec. II we derive the equations governing forward and backward SBS. In Sec. III we solve the linearized equations governing the transient phase of the instability. These equations differ from the linearized equations governing the SBS of an isolated beam [7] because the forward and backward SBS of crossed beams each involve one Stokes wave and two sound waves (rather than one). In Sec. IV we solve the nonlinear equations governing the steady state of the instability. These equations describe the nonlinear competition between forward and backward SBS. In Sec. V we discuss the entire evolution of forward and backward SBS and describe numerical simulations that verify our analysis. We summarize the main results of the paper in Sec. VI.

In the Appendix we show that, in steady state, the equations governing the simultaneous near-forward and near-backward SBS of an isolated beam are equivalent to the equations governing the simultaneous forward and backward SBS of crossed beams. Thus, many results of this paper also apply to the SBS of an isolated beam.

II. GOVERNING EQUATIONS

The SBS of crossed beams is governed by the Maxwell wave equation [1]

$$(\partial_{tt}^2+\omega_e^2-c^2\nabla^2)A_h=-\omega_e^2 n_l A_h \tag{1}$$

for the electromagnetic potential, together with the sound-wave equation [1]

$$(\partial_{tt}^2-c_s^2\nabla^2)n_l=\tfrac{1}{2}c_s^2\nabla^2\langle A_h^2\rangle. \tag{2}$$

The electromagnetic potential $A_h=(v_h/c_s)(m_e/m_i)^{1/2}$ is the quiver speed of electrons in the high-frequency electric field divided by a characteristic speed that is of the order of the electron thermal speed, n_l is the low-frequency electron density fluctuation associated with the sound wave divided by the background electron density, and the $\langle\ \rangle$ signify that only the low-frequency response to the ponderomotive force was retained.

The geometry associated with forward SBS is shown in Fig. 1(a). The forward SBS of beam 1 is subject to matching conditions of the form

$$\omega_1=\omega_f+\omega_{s1},\quad \mathbf{k}_1=\mathbf{k}_f+\mathbf{k}_{s1}, \tag{3}$$

where $(\omega_1,\mathbf{k}_1)$ and $(\omega_f,\mathbf{k}_f)$ satisfy the light-wave dispersion equation $\omega^2=\omega_e^2+c^2k^2$, and $(\omega_{s1},\mathbf{k}_{s1})$ satisfies the sound-wave dispersion equation $\omega^2=c_s^2k^2$. Similar matching conditions apply to the forward SBS of beam 2. Because the sound frequencies depend on the magnitudes of the sound wave vectors, but not on their directions, $\omega_{s2}=\omega_{s1}=\omega_s$.

By substituting the *Ansätze*

$$A_h=[A_1\exp(i\mathbf{k}_1\cdot\mathbf{x}-i\omega_0 t)+A_2\exp(i\mathbf{k}_2\cdot\mathbf{x}-i\omega_0 t)+A_f\exp(i\mathbf{k}_f\cdot\mathbf{x}-i\omega_f t)]+\text{c.c.} \tag{4}$$

and

$$n_l=N_1\exp(i\mathbf{k}_{s1}\cdot\mathbf{x}-i\omega_s t)+N_2\exp(i\mathbf{k}_{s2}\cdot\mathbf{x}-i\omega_s t)+\text{c.c.} \tag{5}$$

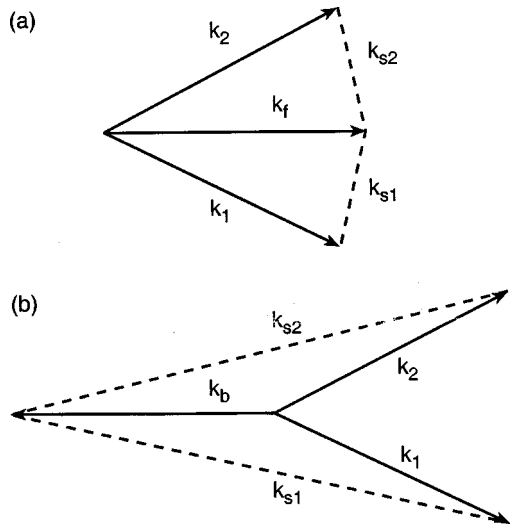

FIG. 1. Geometry associated with the SBS of crossed laser beams. (a) Forward SBS. (b) Backward SBS.

in Eqs. (1) and (2), and making the slowly varying envelope approximation, one can show that

$$\partial_z A_f = i(\omega_e^2/2\omega_0 v_0)(A_1 N_1^* + A_2 N_2^*), \tag{6}$$

$$(\partial_t + \nu_{s1}) N_1^* = -i(\omega_s^2/2\omega_s) A_1^* A_f + \nu_{s1} n^*, \tag{7}$$

$$(\partial_t + \nu_{s2}) N_2^* = -i(\omega_s^2/2\omega_s) A_2^* A_f + \nu_{s2} n^*. \tag{8}$$

In keeping with standard practice, we omitted the time derivative from Eq. (6) because the time taken by the scattered light wave to cross the plasma is short compared to the time taken by the sound waves to respond to the ponderomotive forces that drive them. We also made the approximation that the frequency and group speed of the scattered light wave equal the frequency and group speed v_0 of the pump waves, respectively. In Eqs. (7) and (8), $\nu_{s1} N_1^*$ and $\nu_{s2} N_2^*$ are phenomenological terms that model the Landau damping of the sound waves [12,13], and $\nu_{s1} n^*$ and $\nu_{s2} n^*$ are phenomenological terms than maintain the density fluctuations associated with the sound waves at their common noise level n^* in the absence of instability. Because the Landau-damping rates depend on the magnitudes of the sound wave vectors, but not on their direction, $\nu_{s2} = \nu_{s1} = \nu_s$.

Equations (6)–(8) describe the initial (transient) evolution of SBS. In steady state

$$d_z A_f = \mu_f (|A_1|^2 + |A_2|^2) A_f, \tag{9}$$

where

$$\mu_f = \omega_e^2 \omega_s^2 / 4\omega_0 \omega_s \nu_s v_0. \tag{10}$$

Apart from a factor of $|A_1|^2$ or $|A_2|^2$, μ_f is the spatial growth rate of forward SBS in the strongly damped regime [7]. The forward-scattered intensity $F = |A_f|^2$ satisfies the equation

$$d_z F = 2\mu_f (P_1 + P_2) F, \tag{11}$$

where $P_1 = |A_1|^2$ and $P_2 = |A_2|^2$ are the pump intensities.

The geometry associated with backward SBS is shown in Fig. 1(b). The backward SBS of beam 1 is subject to matching conditions of the form

$$\omega_1 = \omega_b + \omega_{s1}, \quad \mathbf{k}_1 = \mathbf{k}_b + \mathbf{k}_{s1}, \tag{12}$$

where $(\omega_1, \mathbf{k}_1)$ and $(\omega_b, \mathbf{k}_b)$ satisfy the light-wave dispersion equation, and $(\omega_{s1}, \mathbf{k}_{s1})$ satisfies the sound-wave dispersion equation. Similar matching conditions apply to the backward SBS of beam 2. As in forward SBS, $\omega_{s2} = \omega_{s1} = \omega_s$.

By adding to *Ansatz* (4) the term

$$A_b \exp(i\mathbf{k}_b \cdot \mathbf{x} - i\omega_b t) + \text{c.c.} \tag{13}$$

and to *Ansatz* (5) the terms

$$N_1 \exp(i\mathbf{k}_{s1} \cdot \mathbf{x} - i\omega_s t) + N_2 \exp(i\mathbf{k}_{s2} \cdot \mathbf{x} - i\omega_s t) + \text{c.c.} \tag{14}$$

associated with backward SBS, one can show that

$$-\partial_z A_b = i(\omega_e^2/2\omega_0 v_0)(A_1 N_1^* + A_2 N_2^*), \tag{15}$$

$$(\partial_t + \nu_{s1}) N_1^* = -i(\omega_s^2/2\omega_s) A_1^* A_b + \nu_{s1} n^*, \tag{16}$$

$$(\partial_t + \nu_{s2}) N_2^* = -i(\omega_s^2/2\omega_s) A_2^* A_b + \nu_{s2} n^*. \tag{17}$$

As in forward SBS, $\nu_{s2} = \nu_{s1} = \nu_s$. In its transient (linear) phase, backward SBS is independent of forward SBS.

In steady state, the backward-scattered intensity $B = |A_b|^2$ satisfies the equation

$$-d_z B = 2\mu_b (P_1 + P_2) B, \tag{18}$$

where μ_b is given by Eq. (10) and the values of ω_s and ν_s associated with backward SBS. Apart from a factor of $|A_1|^2$ or $|A_2|^2$, μ_b is the spatial growth rate of backward SBS in the strongly damped regime [7].

In the high-gain regime, the intensities of the scattered light waves as they exit the plasma are comparable to the intensities of the pump waves as they enter the plasma and one must account for the depletion of the pump waves within the plasma. In steady state, the pump intensities satisfy the equations

$$d_z P_1 = -2\mu_f F P_1 - 2\mu_b B P_1, \tag{19}$$

$$d_z P_2 = -2\mu_f F P_2 - 2\mu_b B P_2, \tag{20}$$

where we made the approximation that the evolution of the pump waves is one-dimensional. One can verify Eqs. (19) and (20) by applying the principle of power conservation to Eqs. (11) and (18).

III. LINEAR ANALYSIS OF THE TRANSIENT PHASE

The forward SBS of crossed beams consists of two mirror-image processes that share the same Stokes wave and, hence, are governed by the coupled equations (6)–(8). By making the substitutions $\omega_0^{1/2} A_f \to A_f$, $i\omega_e N_1^*/\omega_s^{1/2} \to N_1$, $i\omega_e N_2^*/\omega_s^{1/2} \to N_2$, $i\omega_e n^*/\omega_s^{1/2} \to n$, and $z/v_0 \to z$, one can rewrite these equations as

$$\partial_z A_f = \gamma_{f1} N_1 + \gamma_{f2} N_2, \tag{21}$$

$$(\partial_t + \nu_s) N_1 = \gamma_{f1} A_f + \nu_s n, \tag{22}$$

$$(\partial_t + \nu_s) N_2 = \gamma_{f2} A_f + \nu_s n, \tag{23}$$

where

$$\gamma_{f1} = \omega_e \omega_s |A_1| / 2(\omega_0 \omega_s)^{1/2}, \tag{24}$$

$$\gamma_{f2} = \omega_e \omega_s |A_2| / 2(\omega_0 \omega_s)^{1/2}. \tag{25}$$

A_f is proportional to the action amplitude of the Stokes wave, and N_1 and N_2 are proportional to the action amplitudes of the sound waves. In the absence of damping, γ_{f1} and γ_{f2} are the temporal growth rates of the forward SBS of beams 1 and 2, respectively, in an infinite plasma.

By using the combined amplitudes

$$N_+ = (\gamma_{f1} N_1 + \gamma_{f2} N_2)/\gamma_f, \tag{26}$$

$$N_- = \gamma_f (N_1/\gamma_{f1} - N_2/\gamma_{f2}), \tag{27}$$

where $\gamma_f = (\gamma_{f1}^2 + \gamma_{f2}^2)^{1/2}$, one can rewrite Eqs. (21)–(23) as

$$\partial_z A_f = \gamma_f N_+, \tag{28}$$

$$(\partial_t + \nu_s) N_+ = \gamma_f A_f + \nu_s n_+, \tag{29}$$

$$(\partial_t + \nu_s) N_- = \nu_s n_-, \tag{30}$$

where $n_+ = n(\gamma_{f1} + \gamma_{f2})/\gamma_f$ and $n_- = n\gamma_f(1/\gamma_{f1} - 1/\gamma_{f2})$. Equations (28) and (29) are equivalent to the equations governing the forward SBS of an isolated beam [7] and Eq. (30) is simple. Consequently, the solutions of Eqs. (28)–(30) can be written in the form

$$A_f(z,t) = \int_0^t \int_0^z \nu_s n_+ G_f(z-z', t-t')\, dz'\, dt', \tag{31}$$

$$N_+(z,t) = \int_0^t \int_0^z \nu_s n_+ G_+(z-z', t-t')\, dz'\, dt', \tag{32}$$

$$N_-(z,t) = \int_0^t \int_0^z \nu_s n_- G_-(z-z', t-t')\, dz'\, dt', \tag{33}$$

where the Green functions

$$G_f(z,t) = \gamma_f I_0[2\gamma_f (zt)^{1/2}] \exp(-\nu_s t), \tag{34}$$

$$G_+(z,t) = \gamma_f (t/z)^{1/2} I_1[2\gamma_f (zt)^{1/2}] \exp(-\nu_s t) + \delta(z) \exp(-\nu_s t), \tag{35}$$

$$G_-(z,t) = \delta(z) \exp(-\nu_s t). \tag{36}$$

In Eqs. (34) and (35), I_m is the modified Bessel function of the first kind, of order m. The original amplitudes N_1 and N_2 are determined by Eqs. (32) and (33), and the inversion equations

$$N_1 = (\gamma_{f1}/\gamma_f)[N_+ + (\gamma_{f2}^2/\gamma_f^2) N_-], \tag{37}$$

$$N_2 = (\gamma_{f2}/\gamma_f)[N_+ - (\gamma_{f1}^2/\gamma_f^2) N_-]. \tag{38}$$

Solutions (31)–(33) describe the growth and linear saturation of forward SBS. By analyzing the time dependence of the Green functions, one can show that the linear saturation time

$$t_s \sim \gamma_f^2 z/\nu_s^2. \tag{39}$$

The steady-state limits of solutions (31)–(33) are

$$A_f(z,\infty) = (n_+ \nu_s/\gamma_f)[\exp(\gamma_f^2 z/\nu_s) - 1], \tag{40}$$

$$N_+(z,\infty) = n_+ \exp(\gamma_f^2 z/\nu_s), \tag{41}$$

$$N_-(z,\infty) = n_-. \tag{42}$$

Notice that $\gamma_f^2/\nu_s \nu_0 = \mu_f(|A_1|^2 + |A_2|^2)$, in agreement with Eq. (9). If the interaction length exceeds a few gain lengths, one can model Stokes generation as Stokes amplification with an incident amplitude $A_f(0) = (n_+ \nu_s/\gamma_f)$.

When the gain distance $\gamma_f^2 z/\nu_s \gg 1$, the pump waves are depleted and forward SBS saturates in a time that is short compared to the linear saturation time. One can deduce a scaling law for the nonlinear depletion time from the condition that the intensity amplification factor associated with solution (31) is comparable to the ratio of the incident intensities of the pump and Stokes waves. The result is

$$t_d \propto 1/\gamma_f^2 z. \tag{43}$$

The backward SBS of crossed beams also consists of two mirror-image processes that share a Stokes wave and are governed by Eqs. (21)–(25), with f replaced by b and z replaced by $l - z$. Thus, Eqs. (26)–(43), and the conclusions drawn from them, also apply to backward SBS. Equations (21)–(23) apply to other parametric instabilities driven by crossed pump waves, provided that one type of daughter wave is strongly damped.

IV. NONLINEAR ANALYSIS OF THE STEADY STATE

The simultaneous forward and backward SBS of crossed beams is governed by Eqs. (11) and (18)–(20). By making the substitution $P_1 + P_2 \to P$, one can rewrite these equations as

$$d_z F = 2\mu_f P F, \tag{44}$$

$$-d_z B = 2\mu_b P F, \tag{45}$$

$$d_z P = -2(\mu_f F + \mu_b B) P. \tag{46}$$

Henceforth, the total intensity of the pump waves will be referred to as the pump intensity. Equations (44)–(46) apply to other simultaneous parametric instabilities driven by crossed pump waves, provided that one type of daughter wave is strongly damped. For SBS, $\mu_b = \mu_f = \mu$ [7] and one can use the substitution $2\mu z \to z$ to rewrite Eqs. (44)–(46) in the simple form

$$d_z F = PF, \tag{47}$$

$$-d_z B = PB, \tag{48}$$

$$d_z P = -(F+B)P. \tag{49}$$

The substitutions $F/P(0)\rightarrow F$, $B/P(0)\rightarrow B$, $P/P(0)\rightarrow P$, and $P(0)z\rightarrow z$ nondimensionalize Eqs. (47)–(49), but leave them unchanged in form. Because the solutions of Eqs. (47)–(49) are complicated, it is intructive to review the limiting solutions that apply to forward and backward SBS separately.

A. Forward SBS

In the absence of backward SBS, Eqs. (47)–(49) reduce to

$$d_z F = PF, \tag{50}$$

$$d_z P = -FP. \tag{51}$$

It follows from these equations that

$$P+F = 1+N_f, \tag{52}$$

where $N_f = F(0)$ is incident (noise) intensity of the forward-scattered wave. Since $P \geqslant 0$, it follows from Eq. (52) that

$$S_f \leqslant 1+N_f, \tag{53}$$

where $S_f = F(l)$ is the output (signal) intensity of the forward-scattered wave and l is the gain length of forward SBS. Equation (53) reflects the fact that the signal intensity cannot exceed the total input intensity.

By substituting Eq. (52) in Eq. (50), one can show that

$$(1+N_f)z = \ln\left[\frac{F}{N_f(1+N_f-F)}\right]. \tag{54}$$

Equation (54) determines the interaction distance z required to produce the forward-scattered intensity F. By inverting this equation, one finds that

$$F(\zeta) = \frac{N_f(1+N_f)}{N_f+\exp(-\zeta)}, \tag{55}$$

where $\zeta = (1+N_f)z$. Solution (55) is consistent with Eq. (53).

The normalized intensities of the pump and Stokes waves in a semi-infinite plasma are plotted as functions of the gain distance z in Fig. 2, for the case in which $N_f = 10^{-6}$. As the Stokes intensity increases, the pump intensity decreases, in accordance with Eq. (52). For future reference, notice that the initial growth of the Stokes wave from noise is driven by undepleted pump waves.

B. Backward SBS

In the absence of forward SBS, Eqs. (47)–(49) reduce to

$$-d_z B = PB, \tag{56}$$

$$d_z P = -BP. \tag{57}$$

It follows from these equations that

$$P-B = 1-S_b, \tag{58}$$

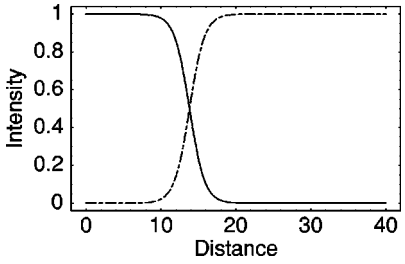

FIG. 2. Normalized intensities plotted as functions of the gain distance for forward SBS in a semi-infinite plasma. The solid line represents the pump waves and the dot-dashed line represents the Stokes wave. For forward SBS the output intensities from a finite plasma depend on the plasma length in the same way that the intensities within a semi-infinite plasma depend on the distance from the plasma boundary.

where $S_b = B(0)$ is the output (signal) intensity of the backward-scattered wave. Since $P \geqslant 0$, it follows from Eq. (58) that

$$S_b \leqslant 1+N_b, \tag{59}$$

where $N_b = B(l)$ is the incident (noise) intensity of the backward-scattered wave and l is the gain length of backward SBS. Equation (59) reflects the fact that the signal intensity cannot exceed the total input intensity.

By substituting Eq. (58) in Eq. (56), one can show that

$$(1-S_b)z = \ln[S_b(1-S_b+B)/B]. \tag{60}$$

The signal intensity is determined by Eq. (60) and the condition $B(l) = N_b$. By inverting Eq. (60), with S_b known, one finds that

$$B(\zeta) = \frac{S_b(1-S_b)}{\exp(\zeta)-S_b}, \tag{61}$$

where $\zeta = (1-S_b)z$. Solution (61), which was first obtained by Tang [14], is consistent with Eq. (59).

The normalized output intensity of the Stokes wave is plotted as a function of the gain length l in Fig. 3(a), for the case in which $N_b = 10^{-6}$. The normalized intensities of the pump and Stokes waves within the plasma are plotted as functions of the gain distance z in Fig. 3(b), for the case in which $N_b = 10^{-6}$ and $l = 30$. Because the pump and Stokes waves propagate in opposite directions, the initial growth of the Stokes wave from noise is driven by depleted pump waves [Fig. 3(b)]. Consequently, when pump depletion is important ($l > 10$), the rate at which the Stokes output intensity increases with gain length is slower for backward SBS [Fig. 3(a)] than for forward SBS (Fig. 2). Backward SBS scatters the pump power less efficiently than forward SBS.

C. Simultaneous forward and backward SBS

When forward and backward SBS occur simultaneously, it follows from Eqs. (47)–(49) that

$$P+F-B = 1+N_f-S_b \tag{62}$$

and

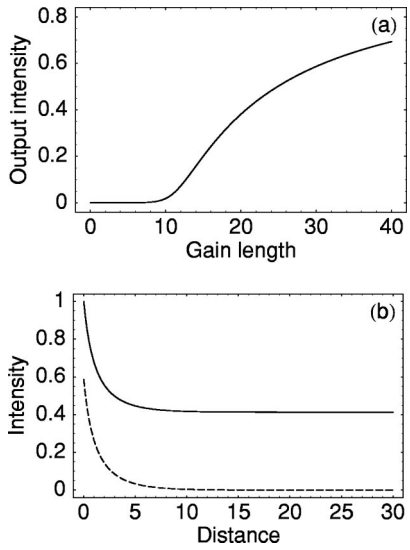

FIG. 3. (a) Normalized output intensity of the Stokes wave plotted as a function of the gain length l for backward SBS. (b) Normalized intensities within the plasma plotted as functions of the gain distance for $l=30$. The solid line represents the pump waves and the dashed line represents the Stokes wave.

$$FB=N_f S_b. \tag{63}$$

Equation (62) is a generalization of equations that apply to the forward and backward instabilities separately, whereas Eq. (63) is peculiar to the combined instability. Since $P \geqslant 0$, it follows from Eq. (62) that

$$S_f+S_b \leqslant 1+N_f+N_b. \tag{64}$$

Equation (64) reflects the fact that the total signal intensity cannot exceed the total input intensity. It follows from Eqs. (63) and (64) that

$$S_f \leqslant N_f+\frac{N_f}{N_f+N_b}, \tag{65}$$

$$S_b \leqslant N_b+\frac{N_b}{N_f+N_b}. \tag{66}$$

By substituting Eqs. (62) and (63) in Eq. (47), one can show that

$$d_z F=(R_+-F)(R_-+F), \tag{67}$$

where

$$\pm 2R_\pm = 1+N_f-S_b \pm [(1+N_f-S_b)^2+4N_f S_b]^{1/2}. \tag{68}$$

It follows from Eq. (67) that

$$(R_++R_-)z=\ln\left[\frac{(R_+-N_f)(R_-+F)}{(R_+-F)(R_-+N_f)}\right]. \tag{69}$$

S_b is determined by Eq. (69) and the condition $B(l)=N_b$, which is equivalent to the condition $F(l)=(N_f/N_b)S_b$. By inverting Eq. (69), with S_b known, one finds that

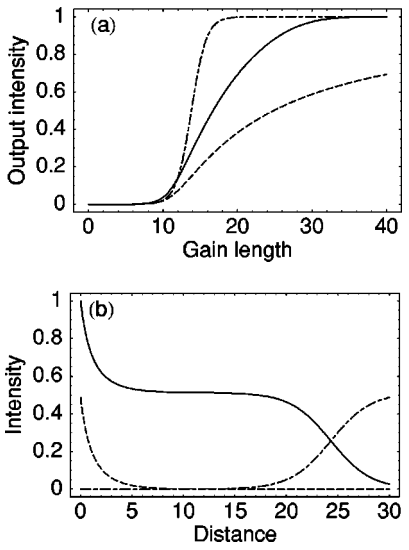

FIG. 4. (a) Normalized output intensities plotted as functions of the SBS gain length l. The forward and backward noise intensities are equal. The solid line represents the total output intensity for the combined instability. For comparison, the dot-dashed and dashed lines represent the output intensities when forward and backward SBS occur separately [Figs. 2 and 3(a), respectively]. (b) Normalized intensities within the plasma plotted as functions of the gain distance for $l=30$. The solid line represents the pump waves, the dot-dashed line represents the forward Stokes wave, and the dashed line represents the backward Stokes wave.

$$F(\zeta)=\frac{R_+(R_-+N_f)\exp(\zeta)-R_-(R_+-N_f)}{(R_-+N_f)\exp(\zeta)+(R_+-N_f)}, \tag{70}$$

where $\zeta=(R_++R_-)z$. Solution (70) is consistent with Eq. (65). For the common case in which $1-S_b \gg N_f$, one can use the approximate roots

$$R_+ \approx 1-S_b+N_f/(1-S_b), \tag{71}$$

$$R_- \approx N_f S_b/(1-S_b), \tag{72}$$

to rewrite Eqs. (69) and (70) as

$$(1-S_b)z \approx \ln\left\{\frac{(1-S_b)[N_f S_b+(1-S_b)F]}{(1-S_b-F)N_f}\right\} \tag{73}$$

and

$$F(\zeta) \approx \frac{N_f(1-S_b)[\exp(\zeta)-S_b]}{N_f\exp(\zeta)+(1-S_b)^2}, \tag{74}$$

respectively, where $\zeta \approx (1-S_b)z$.

The normalized (total) output intensity of the (forward and backward) Stokes waves is plotted as a function of the gain length l in Fig. 4(a), for the case in which $N_b=N_f=10^{-6}$. When pump depletion is unimportant ($l<10$), the Stokes output intensity of the combined instability is the sum of the Stokes output intensities of the forward and backward instabilities. The normalized intensities of the pump and Stokes waves within the plasma are plotted as functions of the gain distance z in Fig. 4(b), for the case in which $N_b=N_f=10^{-6}$ and $l=30$. The initial growth of both Stokes waves from noise is driven by depleted pump waves. Con-

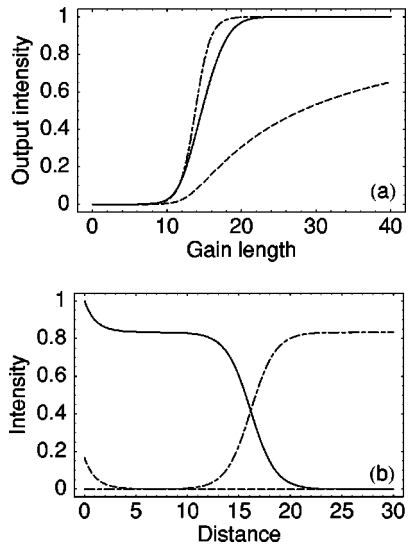

FIG. 5. (a) Normalized output intensities plotted as functions of the SBS gain length l. The forward noise intensity exceeds the backward noise intensity by a factor of 5. The solid line represents the total output intensity for the combined instability. For comparison, the dot-dashed and dashed lines represent the output intensities when forward and backward SBS occur separately. (b) Normalized intensities within the plasma plotted as functions of the gain distance for $l=30$. The solid line represents the pump waves, the dot-dashed line represents the forward Stokes wave, and the dashed line represents the backward Stokes wave.

sequently, when pump depletion is important ($l>10$), the rate at which the Stokes output intensity increases with gain length is slower for the combined instability than for the forward instability [Fig. 4(a)].

In Figs. 2–4 the noise intensities for forward and backward SBS were equal. This choice made possible a fair comparison of the intrinsic scattering efficiencies of the two instabilities. However, the noise intensity for forward SBS is higher than the noise intensity for backward SBS because the action sources that generate the light waves [Eq. (40) for forward SBS and its analog for backward SBS] are inversely proportional to the sound frequencies [15]. To illustrate how this imbalance affects the combined instability, the normalized output intensity of the Stokes waves is plotted as a function of the gain length in Fig. 5(a), for the case in which $N_f=10^{-6}$ and $N_b=2\times10^{-7}$. The normalized intensities of the pump and Stokes waves within the plasma are plotted as functions of the gain distance in Fig. 5(b), for the case in which $N_f=10^{-6}$, $N_b=2\times10^{-7}$, and $l=30$. It is clear from the figures that forward SBS overwhelms backward SBS in steady state.

V. DISCUSSION

Initially, pump depletion is unimportant, and forward and backward SBS grow independently. This linear spatiotemporal growth is described by Eqs. (28)–(30). Since the growth rate $\gamma\propto(\sin\phi)^{1/2}$ [Eqs. (24) and (25)], where 2ϕ is the scattering angle, backward SBS grows more quickly than forward SBS. Since the Landau damping rate $\nu_s\propto\sin(\phi)$ [7], the linear saturation time $t_s\propto1/\sin\phi$ [Eq. (39)]. The nonlinear depletion time $t_d\propto1/\sin\phi$ [Eq. (43)]. Thus, backward SBS saturates before forward SBS, irrespective of the relative importance of dissipation and depletion. The steady-state spatial evolution of backward SBS is described by Eqs. (58) and (61). In the high-gain regime, backward SBS depletes the pump waves significantly [Fig. 3(b)]. Thus, the spatiotemporal growth of forward SBS is driven by pump waves whose intensity varies with distance and Eqs. (31)–(36) do not apply as written. However, by making the substitutions $N_\pm/\gamma_f\rightarrow N_\pm$, $n_\pm/\gamma_f\rightarrow n_\pm$, and $\int_0^z[\gamma_f(z')]^2dz'\rightarrow z$ in Eqs. (28)–(30), one can show that

$$\partial_z A_f=N_+, \tag{75}$$

$$(\partial_t+\nu_s)N_+=A_f+\nu_s n_+, \tag{76}$$

$$(\partial_t+\nu_s)N_-=\nu_s n_-. \tag{77}$$

Since Eqs. (75)–(77) contain no variable coefficients, their solution can be inferred from Eqs. (31)–(36). It follows that the linear saturation and nonlinear depletion times of forward SBS are given by Eqs. (39) and (43), respectively, with $\gamma_f^2 z$ replaced by $\int_0^z[\gamma_f(z')]^2dz'$. The reduction of the gain distance by pump depletion shortens the linear saturation time of forward SBS, but lengthens the nonlinear depletion time. Since the steady-state equations (47)–(49) have a unique solution, the spatial evolution of the combined instability is given by Eqs. (62), (63), and (70), even though forward and backward SBS grow at different rates and saturate at different times. It is clear from Figs. 4 and 5 that the output intensity of the backward Stokes wave is lower in the presence of the forward Stokes wave than in its absence. Thus, the combined instability is characterized by a burst of backward SBS followed by the ascendance of forward SBS.

We checked the analysis of Secs. III and IV by solving the equations governing forward and backward SBS numerically. In our numerical simulations, distance is normalized to the plasma length l_p, time is normalized to the time taken by the light waves to cross the plasma, and intensity is normalized to the incident pump intensity. Consequently, the wave evolution is characterized by the gain parameter $\alpha_f=\gamma_f l_p/v_0$ and the loss parameter $\beta_f=\nu_s l_p/v_0$, together with their analogs for backward SBS. We chose the laser and plasma parameters $\lambda_0=0.35$ μm, $I_1=I_2=2.5\times10^{15}$ W cm^{-2}, $l_p=300$ μm, $n_e=n_i=8.9\times10^{20}$ cm^{-3} (one-tenth critical density), $T_e=5.0$ KeV, and $T_i=1.0$ KeV. The beam-crossing angle $4\phi=40°$. For these physical parameters $\alpha_f=2.3$, $\beta_f=0.35$, $\alpha_b=5.5$, and $\beta_b=2.0$. The ratio of the sound frequencies for forward and backward SBS equals the ratio of the loss parameters, which is 0.18. The results of our simulations are displayed in Fig. 6. In Fig. 6(a), $N_f=10^{-6}$ and $N_b=0$. The output intensity of the forward Stokes wave exhibits weak relaxation oscillations before attaining a steady-state value that is limited by pump depletion. In Fig. 6(b), $N_f=0$ and $N_b=1.8\times10^{-7}$. The output intensity of the backward Stokes wave exhibits weak relaxation oscillations before attaining a steady-state value that is limited by pump depletion. The observed ratio of the nonlinear depletion times for forward and backward SBS is consistent with Eq. (43). In Fig. 6(a), $N_f=10^{-6}$ and $N_b=1.8\times10^{-7}$. As our analysis predicts, backward SBS grows more rapidly than forward SBS and attains a quasisteady state. The

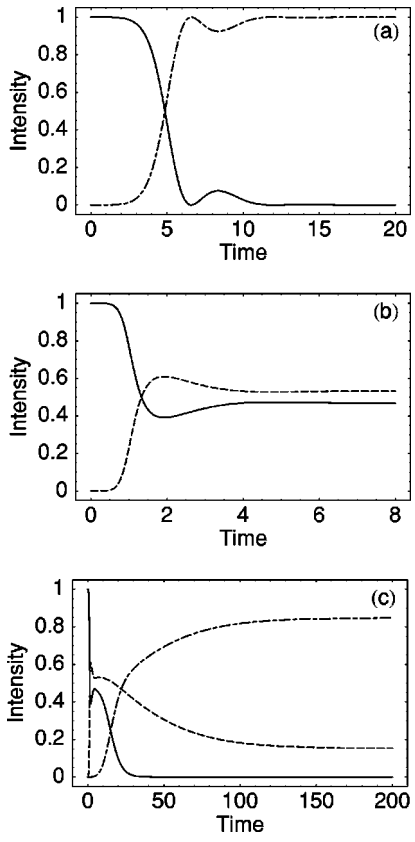

FIG. 6. Normalized output intensities plotted as functions of the normalized time. The solid line represents the pump waves, the dot-dashed line represents the forward Stokes wave, and the dashed line represents the backward Stokes wave. (a) Forward SBS. (b) Backward SBS. (c) Simultaneous forward and backward SBS.

subsequent growth of forward SBS is slowed by the pump depletion associated with backward SBS, but forward SBS eventually suppresses backward SBS. In all three cases, we checked that the final numerical solutions for the wave intensities within the plasma agree with the analytical solutions of Sec. IV.

The analysis and numerical simulations of this paper are based on the standard approximation that the time taken by the light waves to cross the plasma is much shorter than the time taken by the sound waves to respond to the ponderomotive forces that drive them. This approximation is valid when $\alpha \ll 1$ and $\beta \ll 1$. Although these conditions are satisfied for a wide range of physical parameters, they are not satisfied for the physical parameters listed here. Consequently, we restored the time derivatives to the light-wave equations [Eqs. (6) and (15), and their analogs for the pump waves] and used the method of characteristics to solve the resulting equations numerically. For forward SBS, the output intensities are delayed by 1 transit time, but are otherwise identical to those displayed in Fig. 6(a). For backward SBS the relaxation oscillations are more pronounced because the light waves take a finite time to respond to the sound waves. The first maximum of the Stokes intensity exceeds the incident pump intensity by a factor of 1.2. However, after this initial burst of backward Stokes radiation, the evolution of the output intensities is similar to that displayed in Fig. 6(b). In particular, the steady-state output intensities are identical. The combined instability also exhibits a burst of backward Stokes radiation, after which the evolution of the output intensities is similar to that displayed in Fig 6(c). In steady state, the output intensities are identical.

The major theme of Sec. IV and the preceding discussion is that forward and backward SBS coexist and compete for the pump energy. One should remember that several other processes also coexist and modify this competition. These processes include double SBS [9], which is made possible by a sound wave whose wave vector is the sum of the pump wave vectors, and the transfer of energy between the pump waves [16–24] and the Bragg scattering of the pump waves [17], both of which are made possible by a sound wave whose wave vector is the difference of the pump wave vectors. While much remains to be learned about crossed-beam interactions, one should note that the second process transfers energy from one pump wave to the other, but conserves the total pump energy. Consequently, it does not impede the combined SBS instability [Eqs. (44)–(46)].

VI. SUMMARY

In this paper, we studied in detail the simultaneous forward and backward SBS of crossed laser beams. We obtained analytical solutions for the linearized equations governing the transient phase of the instability [Eqs. (21)–(23)] and the nonlinear equations governing the steady state [Eqs. (47)–(49)]. In their transient phases, forward and backward SBS grow independently. Initially, backward SBS grows more quickly than forward SBS. As the backward Stokes wave grows, it depletes the pump waves and slows the growth of the forward Stokes wave. In steady state, forward SBS dominates the combined instability, because the forward Stokes wave has a higher noise intensity from which to grow and forward SBS scatters the pump power more efficiently.

In the Appendix we show that the equations governing the simultaneous near-forward and near-backward SBS of an isolated beam are equivalent to the equations governing the simultaneous forward and backward SBS of crossed beams. Thus, the results of this paper also apply to the SBS of an isolated beam.

ACKNOWLEDGMENTS

We acknowledge useful discussions with R. E. Giacone and A. V. Kanaev. This work was supported by the National Science Foundation under Contract No. PHY-9415583, the Department of Energy (DOE) Office of Inertial Confinement Fusion under Cooperative Agreement No. DE-FC03-92SF19460, the University of Rochester, and the New York State Energy Research and Development Authority.

APPENDIX: FORWARD AND BACKWARD SBS OF AN ISOLATED LASER BEAM

In this appendix we show that the equations governing the simultaneous forward and backward SBS of an isolated beam are equivalent to the equations governing the simultaneous forward and backward SBS of crossed beams. The geometry associated with the forward SBS of an isolated beam is shown in Fig. 7(a). Each forward-scattering process is subject to matching conditions of the form

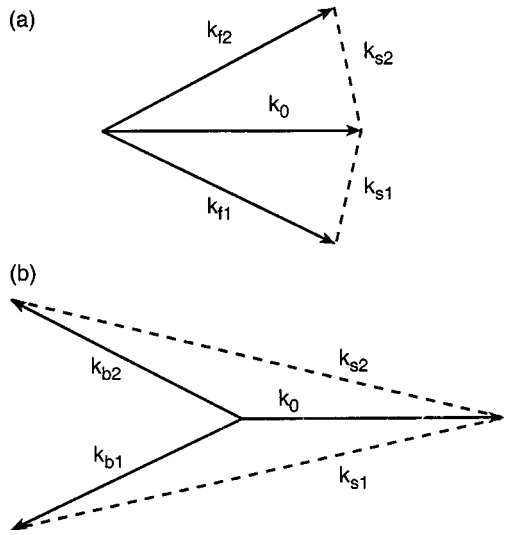

FIG. 7. Geometry associated with the SBS of an isolated laser beam. (a) Near-forward SBS. (b) Near-backward SBS.

$$\omega_0=\omega_f+\omega_s\,,\quad \mathbf{k}_0=\mathbf{k}_f+\mathbf{k}_s\,, \tag{A1}$$

where $(\omega_0,\mathbf{k}_0)$ and $(\omega_f,\mathbf{k}_f)$ satisfy the light-wave dispersion equation $\omega^2=\omega_e^2+c^2k^2$, and $(\omega_s,\mathbf{k}_s)$ satisfies the sound-wave dispersion equation $\omega^2=c_s^2k^2$. Because the frequencies of the daughter waves depend on the magnitude of their wave vectors, but not on their directions, $\omega_{f2}=\omega_{f1}=\omega_f$ and $\omega_{s2}=\omega_{s1}=\omega_s$.

By substituting the *Ansätze*

$$A_h=[A_0\exp(i\mathbf{k}_0\cdot\mathbf{x}-i\omega_0t)+A_{f1}\exp(i\mathbf{k}_{f1}\cdot\mathbf{x}-i\omega_ft)+A_{f2}\exp(i\mathbf{k}_{f2}\cdot\mathbf{x}-i\omega_ft)]+\text{c.c.} \tag{A2}$$

and

$$n_l=N_1\exp(i\mathbf{k}_{s1}\cdot\mathbf{x}-i\omega_st)+N_2\exp(i\mathbf{k}_{s2}\cdot\mathbf{x}-i\omega_st)+\text{c.c.} \tag{A3}$$

into Eqs. (1) and (2), and making the slowly varying envelope approximation, one can show that each forward-scattering process is governed by equations of the form

$$\partial_zA_f=i(\omega_e^2/2\omega_0v_0)A_0N^*, \tag{A4}$$

$$(\partial_t+\nu_s)N^*=-i(\omega_s^2/2\omega_s)A_0^*A_f+\nu_sn^*. \tag{A5}$$

In Eq. (A5), ν_sN^* is a phenomenological term that models the Landau damping of the sound wave and ν_sn^* is a phenomenological term that maintains the density fluctuations associated with the sound wave at their noise level n^* in the absence of instability. Because the Landau-damping rates depend on the magnitudes of the sound wave vectors, but not on their directions, $\nu_{s2}=\nu_{s1}=\nu_s$. By making the substitutions $\omega_0^{1/2}A_f\rightarrow A_f$, $i\omega_eN^*/\omega_s^{1/2}\rightarrow N$, $i\omega_en^*/\omega_s^{1/2}\rightarrow n$, and $z/v_0\rightarrow z$, one can rewrite Eqs. (A4) and (A5) as

$$\partial_zA_f=\gamma_fN, \tag{A6}$$

$$(\partial_t+\nu_s)N=\gamma_fA_f+\nu_sn, \tag{A7}$$

where

$$\gamma_f=\omega_e\omega_s|A_0|/2(\omega_0\omega_s)^{1/2}. \tag{A8}$$

Equations (A6) and (A7) are equivalent to Eqs. (28) and (29), the solution of which was described in the text.

Equations (A4) and (A5) describe the transient evolution of forward SBS. In steady state,

$$d_zA_f=\mu_f|A_0|^2A_f\,, \tag{A9}$$

where

$$\mu_f=\omega_e^2\omega_s^2/4\omega_0\omega_s\nu_sv_0\,. \tag{A10}$$

Notice that $\mu_f|A_0|^2=\gamma_f^2/\nu_sv_0$, in agreement with Eqs. (A6)–(A8). It follows from Eq. (A9) that the forward-scattered intensities $F_1=|A_{f1}|^2$ and $F_2=|A_{f2}|^2$ satisfy the equations

$$d_zF_1=2\mu_fPF_1\,, \tag{A11}$$

$$d_zF_2=2\mu_fPF_2\,, \tag{A12}$$

where $P=|A_0|^2$ is the pump intensity.

The geometry associated with the backward SBS of an isolated beam is shown in Fig. 7(b). Each backward-scattering process is subject to matching conditions of the form

$$\omega_0=\omega_b+\omega_s\,,\quad \mathbf{k}_0=\mathbf{k}_b+\mathbf{k}_s\,, \tag{A13}$$

where $(\omega_0,\mathbf{k}_0)$ and $(\omega_b,\mathbf{k}_b)$ satisfy the light-wave dispersion equation, and $(\omega_s,\mathbf{k}_s)$ satisfies the sound-wave dispersion equation. As in forward SBS, $\omega_{b2}=\omega_{b1}=\omega_b$ and $\omega_{s2}=\omega_{s1}=\omega_s$.

By adding to *Ansatz* (A2) the terms

$$A_{b1}\exp(i\mathbf{k}_{b1}\cdot\mathbf{x}-i\omega_bt)+A_{b2}\exp(i\mathbf{k}_{b2}\cdot\mathbf{x}-i\omega_bt)+\text{c.c.}, \tag{A14}$$

and to *Ansatz* (A3) the terms

$$N_1\exp(i\mathbf{k}_{s1}\cdot\mathbf{x}-i\omega_st)+N_2\exp(i\mathbf{k}_{s2}\cdot\mathbf{x}-i\omega_st)+\text{c.c.} \tag{A15}$$

associated with backward SBS, one can show that each backward-scattering process is governed by equations of the form

$$-\partial_zA_b=i(\omega_e^2/2\omega_0v_0)A_0N^*, \tag{A16}$$

$$(\partial_t+\nu_s)N^*=-i(\omega_s^2/2\omega_s)A_0^*A_b+\nu_sn^*. \tag{A17}$$

As in forward SBS, $\nu_{s2}=\nu_{s1}=\nu_s$. It follows from Eqs. (A16) and (A17) that the transient evolution of backward SBS is governed by Eqs. (A6)–(A8), with f replaced by b and z replaced by $l-z$. Equations (A6) and (A7) apply to other parametric instabilities driven by an isolated pump wave provided that one type of daughter wave is strongly damped. In steady state, the backward-scattered intensities $B_1=|A_{b1}|^2$ and $B_2=|A_{b2}|^2$ satisfy the equations

$$-d_zB_1=2\mu_bPB_1\,, \tag{A18}$$

$$-d_zB_2=2\mu_bPB_2\,, \tag{A19}$$

where μ_b is given by Eq. (A10), with f replaced by b.

In the high-gain regime, the intensities of the scattered waves as they exit the plasma are comparable to the intensity of the pump wave as it enters the plasma, and one must account for the depletion of the pump wave within the plasma. In steady state, the pump intensity satisfies the equation

$$d_z P = -2\mu_f(F_1+F_2)-2\mu_b(B_1+B_2). \tag{A20}$$

By making the substitutions $F=F_1+F_2$ and $B=B_1+B_2$ in Eqs. (A11), (A12), (A18), (A19), and (A20), one can show that the simultaneous forward and backward SBS of an isolated beam is governed by the equations

$$d_z F = 2\mu_f PF, \tag{A21}$$

$$-d_z B = 2\mu_b PB, \tag{A22}$$

$$d_z P = -2(\mu_f F+\mu_b B)P. \tag{A23}$$

Equations (A21)–(A23) are equivalent to Eqs. (44)–(46), the solution of which was described in the text. It is clear from the derivation of Eqs. (A21)–(A23) that one can interpret F as the intensity scattered forward over the entire range of angles for which propagation in the z direction is a reasonable approximation, and one can interpret B as the intensity scattered backward over the entire range of angles for which propagation in the $-z$ direction is a reasonable approximation. Equations (A21)–(A23) apply to other parametric instabilities driven by an isolated pump wave, provided that one type of daughter wave is strongly damped. For SBS, $\mu_b=\mu_f=\mu$ [7] and one can use the substitution $2\mu z\to z$ to rewrite Eqs. (A21)–(A23) in the form of Eqs. (47)–(49).

[1] W. L. Kruer, *The Physics of Laser Plasma Interactions* (Addison-Wesley, Redwood City, CA, 1988).

[2] R. L. McCrory and J. M. Soures, in *Laser-Induced Plasmas and Applications*, edited by L. J. Radziemski and D. A. Cremers (Dekker, New York, 1989), p. 207.

[3] J. D. Lindl, Phys. Plasmas **2**, 3933 (1995).

[4] M. R. Amin, C. E. Capjack, P. Frycz, W. Rozmus, and V. T. Tikhonchuk, Phys. Rev. Lett. **71**, 81 (1993).

[5] M. R. Amin, C. E. Capjack, P. Frycz, W. Rozmus, and V. T. Tikhonchuk, Phys. Fluids B **5**, 3748 (1993).

[6] C. J. McKinstrie, R. Betti, R. E. Giacone, T. Kolber, and J. S. Li, Phys. Rev. E **50**, 2182 (1994).

[7] R. E. Giacone, C. J. McKinstrie, and R. Betti, Phys. Plasmas **2**, 4596 (1995); **5**, 1218 (1998).

[8] C. J. McKinstrie, J. S. Li, and A. V. Kanaev, Phys. Plasmas **4**, 4227 (1997).

[9] A. A. Zozulya, V. P. Silin, and V. T. Tikhonchuk, Zh. Éksp. Teor. Fiz. **92**, 788 (1987) [Sov. Phys. JETP **65**, 443 (1987)].

[10] D. F. DuBois, B. Bezzerides, and H. A. Rose, Phys. Fluids B **4**, 241 (1992).

[11] C. J. McKinstrie and M. V. Goldman, J. Opt. Soc. Am. B **9**, 1778 (1992).

[12] For Maxwellian velocity distributions, see C. J. McKinstrie, R. E. Giacone, and E. A. Startsev, Phys. Plasmas **6**, 463 (1999), and references therein.

[13] For non-Maxwellian velocity distributions, see B. B. Afeyan, A. E. Chou, J. P. Matte, R. P. J. Town, and W. L. Kruer, Phys. Rev. Lett. **80**, 2322 (1998), and references therein.

[14] C. L. Tang, J. Appl. Phys. **37**, 2945 (1966).

[15] R. L. Berger, E. A. Williams, and A. Simon, Phys. Fluids B **1**, 414 (1989).

[16] W. L. Kruer, S. C. Wilks, B. B. Afeyan, and R. K. Kirkwood, Phys. Plasmas **3**, 382 (1996).

[17] V. V. Eliseev, W. Rozmus, V. T. Tikhonchuk, and C. E. Capjack, Phys. Plasmas **3**, 2215 (1996).

[18] C. J. McKinstrie, J. S. Li, R. E. Giacone, and H. X. Vu, Phys. Plasmas **3**, 2686 (1996).

[19] C. J. McKinstrie, V. A. Smalyuk, R. E. Giacone, and H. X. Vu, Phys. Rev. E **55**, 2044 (1997).

[20] C. J. McKinstrie, A. V. Kanaev, V. T. Tikhonchuk, R. E. Giacone, and H. X. Vu, Phys. Plasmas **5**, 1142 (1998).

[21] B. I. Cohen, B. F. Lasinski, A. B. Langdon, E. A. Williams, K. B. Wharton, R. K. Kirkwood, and K. G. Estabrook, Phys. Plasmas **5**, 3408 (1998).

[22] R. K. Kirkwood, B. B. Afeyan, W. L. Kruer, B. J. MacGowan, J. D. Moody, D. S. Montgomery, D. M. Pennington, T. L. Weiland, and S. C. Wilks, Phys. Rev. Lett. **76**, 2065 (1996).

[23] A. K. Lal, K. A. Marsh, C. Joshi, C. E. Clayton, C. J. McKinstrie, J. S. Li, and T. W. Johnston, Phys. Rev. Lett. **78**, 670 (1997).

[24] K. B. Wharton, R. K. Kirkwood, S. H. Glenzer, K. G. Estabrook, B. B. Afeyan, B. I. Cohen, J. D. Moody, and C. Joshi, Phys. Rev. Lett. **81**, 2248 (1998).